ImmunoTargets and Therapy

Dovepress
Taylor & Francis Group

Open Access Full Text Article

ORIGINAL RESEARCH

A Critical Role of DC-SIGN^{+} Tumor-Associated Macrophages in Colorectal Cancer Immune Evasion and Progression via BCL-3-Mediated PD-L1 Expression

Jianfeng Zhang[1,*], Yifan Zhao[1,*], Xingchao Wang[1,2], Chuang Miao[1], Wangcheng Xu[1], Chunhua Wan[3], Baoying Hu[1], Fei Qian[1]

[1]Department of General Surgery, Affiliated Hospital of Nantong University & Department of Immunology, School of Medicine, Nantong University, Nantong, 226001, People's Republic of China; [2]Department of General Surgery Heze City Hospital, Heze, 274000, People's Republic of China; [3]School of Public Health, Nantong University, Nantong, 226001, People's Republic of China

*These authors contributed equally to this work

Correspondence: Fei Qian; Baoying Hu, Department of General Surgery, Affiliated Hospital of Nantong University & Department of Immunology, School of Medicine, Nantong University, Nantong, 226001, People's Republic of China, Tel +86 513 8505 1893, Email qianfeint@163.com; huby86@ntu.edu.cn

Background: Tumor-associated macrophages (TAMs) play a pivotal role in facilitating tumor immune escape in colorectal cancer (CRC). C-type lectin Dendritic Cell-Specific ICAM-Grabbing Nonintegrin (DC-SIGN) is variably expressed in TAMs in tumor tissues. However, its role in CRC progression remains poorly defined.

Methods: We analyzed The Cancer Genome Atlas (TCGA) data and an independent CRC cohort to evaluate the prognostic significance of DC-SIGN^{high} TAMs. Immunofluorescence and flow cytometry were used to characterize DC-SIGN expression in CRC tissues. RNA sequencing and bioinformatics analyses were performed on sorted DC-SIGN^{high} and DC-SIGN^{low} TAMs. Functional assays using THP-1–derived macrophages and primary TAMs were conducted to examine how DC-SIGN regulates PD-L1 expression via the transcription factor BCL-3.

Results: DC-SIGN was specifically expressed in TAMs within CRC tissues and was associated with increased stromal and immune cell infiltration. DC-SIGN expression correlated with worsened prognosis in CD8^{high}, but not CD8^{low}, patients with CRC across two independent cohorts, and served as an independent predictor of unfavorable survival in CD8^{high} CRC. Transcriptomic profiling revealed that DC-SIGN^{high} TAMs exhibited distinct immune-related pathways, including marked upregulation of PD-L1 and PD-L1 immune checkpoint pathway. Mechanistically, Lewis^{x}-ligated DC-SIGN upregulated PD-L1 expression at both mRNA and protein levels through BCL-3, which directly bound to the PD-L1 promoter.

Conclusion: The DC-SIGN/BCL-3 axis in TAMs drives PD-L1 expression and contributes to CRC immune evasion. Targeting DC-SIGN^{+} TAMs may represent a promising therapeutic strategy to reprogram the tumor microenvironment (TME) and improve the efficacy of immunotherapy in CRC.

Plain Language Summary: Colorectal cancer is one of the most common cancers, and while the immune system is designed to recognise and destroy cancer cells, tumours can develop ways to avoid this attack. In this study, we investigated immune cells called macrophages, which normally protect the body but can be reprogrammed inside tumours to support cancer growth. We found that a molecule called DC-SIGN is present on many of these macrophages in colorectal cancer and that patients with higher levels of these DC-SIGN–positive macrophages had poorer outcomes, particularly when their tumours also contained many cancer-fighting T cells. By studying these cells in detail, we discovered that DC-SIGN increases the production of PD-L1, a protein that blocks T cells from killing cancer cells. We also showed that DC-SIGN uses another protein, BCL-3, as a switch to turn on PD-L1. These findings reveal a new way that colorectal cancer avoids the immune system and suggest that targeting DC-SIGN may help improve immunotherapy, a treatment that boosts the body's natural defences against cancer.

Received: 20 August 2025
Accepted: 2 December 2025
Published: 10 December 2025

Keywords: colorectal cancer, tumor-associated macrophages, C-type lectin dendritic cell-specific ICAM-grabbing nonintegrin, programmed cell death ligand-1, BCL-3, immune evasion

Graphical Abstract

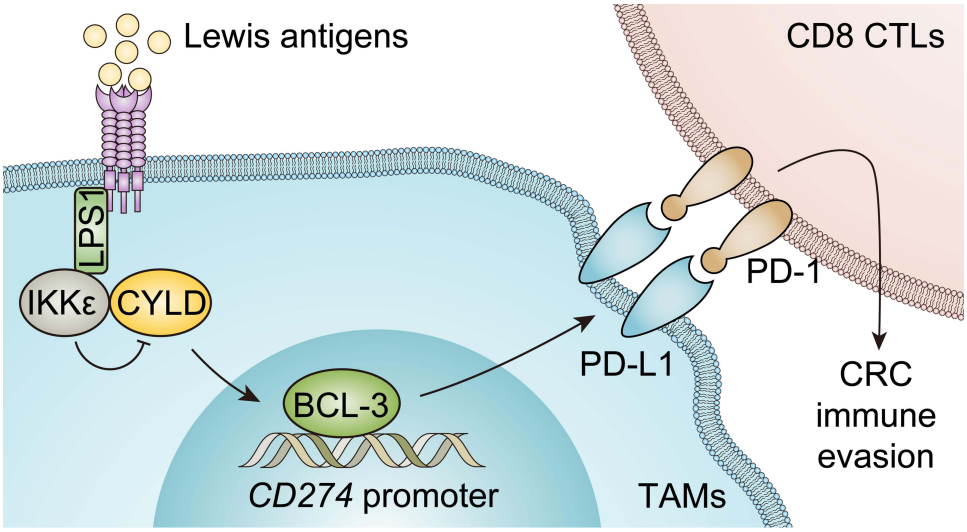

Introduction

The Colorectal cancer (CRC) is the third most common malignancy and a leading cause of cancer-related deaths worldwide.[1,2] According to 2023 data from the United States, the incidence of CRC among adults under 50 is rising by nearly 2% per year.[3] While this increase is partially due to improved awareness and early screening efforts, it remains a concerning trend. Currently, the primary treatment for CRC is surgical resection during the early stages, which significantly improves prognosis. Additionally, immune checkpoint inhibitors (ICIs) can be effective for metastatic CRC with microsatellite-instability-high (MSI-H) characteristics.[4–6] However, the response rate in Microsatellite Stable (MSS) CRC (0.12) remains significantly lower compared to other tumors, such as non-small cell lung cancer (4.67).[7]

The tumor immune microenvironment (TIME) plays a crucial role in evading immune surveillance and promoting tumor growth and metastasis.[8,9] A deeper understanding of the TIME is therefore essential for guiding novel immunotherapeutic strategies. Within the TIME, TAMs are key players that fuel tumor progression and suppress anti-tumor immunity.[10] This can be achieved by the expression of tumor-promoting cytokines such as Interleukin-6 (IL-6),[11] and crucial immune checkpoint proteins, such as PD-L1, which directly inhibits effector T cell function.[12,13] Notably, TAMs exhibit marked functional plasticity, dynamically shifting between pro-inflammatory (M1-like) and immunosuppressive (M2-like) phenotypes.[14] This plasticity underscores the necessity of moving beyond broad categorizations to study distinct TAM subtypes and their specific roles in shaping the TIME.

Dendritic cell-specific intercellular adhesion molecule (ICAM)-3-grabbing non-integrin (DC-SIGN, encoded by *Cd209* gene) is a pattern recognition receptor that recognizes non-sialylated Lewis^x and Lewis^y glycans.[15] Primarily expressed in dendritic cells (DCs) and macrophages, DC-SIGN plays a pivotal role in various immune processes, including dendritic cell adhesion and migration, inflammatory response, T cell activation, and tumor immune evasion.[16] Recent studies have shown that DC-SIGN$^+$ TAMs can facilitate immune escape in gastric, lung, and breast cancers.[17–19] Although the clinical significance of DC-SIGN$^+$ TAMs in CRC remains largely unexplored, studies have shown that DC-

SIGN ligands, including N-glycanated proteins, are specifically enriched in human CRC tissues.[20,21] Furthermore, targeting these glycoproteins may boost anti-tumor immunity to induce CRC regression.[22] These studies highlight DC-SIGN^{+} TAMs as a potential immunotherapeutic target of CRC.

In this study, we identified that DC-SIGN is predominantly expressed in TAMs in CRC specimens. Immunofluorescence and flow cytometry analyses revealed differential expression of DC-SIGN in cancerous versus adjacent non-cancerous tissues, and its prognostic merit in determining CRC outcomes. High DC-SIGN expression is linked to a tumor-promoting environment, offering a new perspective on CRC immunotherapy targeting DC-SIGN. Additionally, RNA-seq and bioinformatics analysis showed that DC-SIGN^{high} TAMs are highly enriched with the immune checkpoint protein PD-L1. These findings suggest that targeting DC-SIGN^{high} TAMs holds therapeutic potential for developing novel immune therapies against CRC.

Materials and Methods

Clinical Samples

Tumor tissues from 246 patients with CRC (Nantong cohort) were collected at the Affiliated Hospital of Nantong University (Nantong, Jiangsu, China). Samples were obtained with informed consent, following a protocol approved by the Ethics Committee and Institutional Review Board (Ethics number 2020-K091-01). A total of 246 colorectal adenocarcinoma (COAD) tissues and 30 corresponding non-cancerous adjacent tissues (at least 5 cm from the tumor margin) were gathered. Fresh tissue specimens for flow cytometry analysis were also sourced from patients undergoing curative resection for colorectal cancer at the same hospital. All COAD tissues and adjacent non-cancerous tissues selected for this study underwent pathological examination, and the patients included had not received radiotherapy, chemotherapy, or immunotherapy prior to surgery.

Cell Culture, Treatment, and siRNA Transfection

The human monocytic cell line (THP-1) was purchased from Cell bank of Chinese Academy of Science (Shanghai, China) and cultured in RPMI-1640 medium (Gibco, USA) supplemented with 10% fetal bovine serum (FBS, Gibco) and 1% penicillin/streptomycin (#15070063, Thermo Fisher Scientific). Cells were confirmed to be free of Mycoplasma contamination using a Mycoplasma detection kit (#4460626, Thermo Fisher Scientific) and were maintained in a humidified incubator at 37°C with 5% CO□. THP-1 cells (5×10^5 cells/well) were seeded into 6-well plates and treated with 100 ng/mL phorbol 12-myristate 13-acetate (PMA, Sigma) for 24 hours to induce differentiation into M0 macrophages. Subsequently, the cells were treated with FBS-free RPMI-1640 medium for 24h and then treated with 20 ng/mL IL-4 (#AF200-04-20UG, PeproTech) and IL-13 (#AF200-13-20UG, PeproTech) for 48 hours to induce M2-like macrophages. Cells were incubated with 10 μg/mL Lewis^X (Le^X, abs42020565, Absin) for an additional 36 hours.

For siRNA transfection, THP-1 cells were first treated with 100 ng/mL PMA for 24 h to induce cell attachment. Subsequently, the cells were transfected with either control siRNA or *BCL3* siRNA SMARTPool (Dharmacon, Lafayette, CO, USA) using Lipofectamine RNAiMAX transfection reagent, following the manufacturer's protocol. After 24 h of transfection, the cells were stimulated with 20 ng/mL IL-4 and IL-13 to induce M2 macrophage polarization, followed by Le^X treatment. Cells were harvested 48 h post M2 induction for RT-qPCR and flow cytometry analysis.

Preparation of Single Cell Suspension

A single-cell suspension was prepared using the Miltenyi Human Tumor Dissociation Kit (#130-095-929, Miltenyi) according to the manufacturer's instructions. Briefly, fresh human colorectal adenocarcinoma tissues were placed on ice, thoroughly washed with PBS, and cut into small pieces approximately 2–4 mm in diameter. The tissues were then resuspended in 5 volumes of the enzyme cocktail and digested at 37 °C on the MACS mix Tube Rotator for 30 minutes. After digestion, the cell suspension was filtered through a 70 μm cell strainer into a 50 mL conical tube. The filtered suspension was centrifuged at 4 °C, 300×g for 7 minutes, resuspended in PBS buffer, and centrifuged again under the same conditions. Red blood cells were removed using a red blood cell lysis buffer (#R1010, Solarbio), following the manufacturer's protocol. The resulting single-cell suspension was then ready for subsequent experiments.

Flow Cytometry Analysis and Fluorescence Activated Cell Sorting

Flow cytometry analysis was performed as previously described.[23] Briefly, single-cell suspension was washed twice with the staining buffer and centrifuged at 1500 rpm for 5 minutes, and then resuspended in the staining buffer. 100 μL of the cell suspension (less than 1×10^6 cells) were aliquoted into a light-protected EP tube, mixed with appropriate volume of primary antibodies according to the antibody instructions, and incubated on ice in dark for 30 minutes. The cell samples were washed using 1mL of the staining buffer for three times in dark. Finally, the cell samples were resuspended in 100 μL of staining buffer and subjected to cell sorting on a BD FACS Aria Fusion cell sorter (BD Biosciences, San Jose, CA). Antibodies used in flow cytometry were as follows: FITC-CD68 (BD Biosciences, 562117), APC-Cy™7-CD45 (BD Biosciences, 561863), APC-DC-SIGN (9E9A8, BioLegend, USA), PE-Cyanine7-PD-L1(MIH1, 25–5983-42, Invitrogen, Waltham, MA, USA).

Immunohistochemistry and Immunofluorescence

All human colorectal cancer and adjacent non-cancerous tissues were processed into paraffin-embedded tissue microarrays using a standard paraffin-embedding protocol. Immunohistochemical and immunofluorescence analyses were performed on these microarrays as previously described.[24]

RNA-Sequencing (RNA-Seq) and Real-Time Quantitative Polymerase Chain Reaction (RT-qPCR)

Immediately after sorting, single cell suspension was lysed with RNA lysis buffer (R401-01, Vazyme), then shipped on dry ice for RNA-seq analysis. Utilizing the Smart-seq2 technology, full-length transcriptome amplification of poly(A)-tailed mRNA is performed, followed by library construction, high-throughput sequencing, and bioinformatics analysis.

For RT-qPCR, total RNA was extracted using the Trizol reagent (Sigma) and then subjected to RT-qPCR experiments using the StepOne Plus RealTime PCR System (Applied Biosystems, USA). The qPCR reactions were performed using AceQ qPCR SYBR Green Master Mix (Vazyme, China). The primers used in RT-qPCR were as follows: *CD209*, 5'-AAC AGC TGA GAG GCC TTG GA-3', and 5'-GGG ACC ATG GCC AAG ACA-3'; *PD-L1*, 5'-TAT GGT GGT GCC GAC TAC AA-3', and 5'-CTT TGG TTG ATT TTG TTG TAT G-3'; *BCL3*, 5'-ACA CCG AGT GCC AAG AAA CC-3', and 5'-CTT AAT GTC CAC TGC GTC GAT G-3'; *β-actin*, 5'-GCA CAG AGC CTC GCC TT-3', and 5'-GTT GTC GAC GAC GAG CG-3'.

Chromatin Immunoprecipitation Quantitative PCR (ChIP-qPCR)

ChIP assay was performed using an enzymatic ChIP assay kit (P2083S, Beyotime, Shanghai). Briefly, THP-1 cells were first differentiated by stimulation with 100 ng/mL and 20 ng/mL IL-4/IL-13. Cells were then treated with or without 10 μg/mL Le^X for 3h before crosslinking with 1% formaldehyde for 10 minutes at room temperature. After glycine quenching, cells were harvested and nucleoli were isolated using hypotonic buffers. Chromatin DNA was sheared using 20 U/μL MNase in 100 μL enzymatic digestion buffer at 37 °C into 150–700 bp fragments. 10 μg chromatin DNA was incubated with 2 μg isotype IgG or anti-BCL-3 antibody in 200 μL ChIP buffer (23959-1-AP, Proteintech) at 4 °C overnight, followed by immunocomplex pull down using 30μL Protein A/G Magnetic Beads. Both input and ChIP DNA samples were reverse cross-linked and using phenol-chloroform ethanol precipitation. The resultant DNA were subjected to RT-qPCR using the StepOne Plus RealTime PCR System. BCL-3 ChIP primers are 5'-CTGGATTTGCTGCCTTGGG-3' and 5'- GAAGCTGCGCAGAACTGG-3'.

Bioinformatic Analysis

The colorectal adenocarcinoma (COAD) gene expression data and clinical data were downloaded from TCGA official website (http://gdc.cancer.gov). Gene expression were expressed as $\log_2$(FPKM+1). We used R software (v.4.2.3) and the R package Limma to analyze differentially expressed genes (DEGs) between DC-$SIGN^{high}$ TAMs and DC-$SIGN^{low}$ TAMs in the TCGA cohort. Volcano plots and heatmaps were then created using the R packages ggplot2 and pheatmap, respectively. The screening criteria for DEGs were P value < 0.05 and absolute value of Log2FC > 1. Gene set

enrichment analysis (GSEA) was conducted using GSEA software (v.4.0). Immune cell infiltration was estimated using the CIBERSORT algorithm.[25]

Single-cell RNA-seq data were obtained from publicly available GEO datasets (GSE132257 and GSE144735) and processed using the Seurat package (version 5.3.0) following standard analysis workflows. Macrophages were identified based on co-expression of two pan-macrophage markers, CD68 and LYZ. The relationships among CD209, CD206, and PD-L1 expression within the macrophage population were subsequently analyzed using their log-transformed, normalized UMI counts.

Statistical Analysis

Data analysis was performed using SPSS (v.20.0), GraphPad Prism 8.3, and R (v.4.2.3) software. Survival analysis was conducted using the R survival package. Patients were stratified into groups based on either median or optimized DC-SIGN expression levels. Kaplan-Meier curves were plotted to visualize survival differences, and Cox proportional hazards regression was used to quantify the association. The relationship between gene expression and clinical pathological characteristics was analyzed using Pearson's chi-square test. Results are presented as means ± SEM, where * $P < 0.05$, ** $P < 0.01$ and *** $P < 0.001$ indicate statistically significant differences.

Results

DC-SIGN Expression is Associated with Immune Microenvironment in COAD

To decipher the role of DC-SIGN in CRC TIME and progression, we analyzed its expression across multiple cancer types in comparison to corresponding non-tumorous tissues. A pan-cancer analysis using TCGA data revealed that DC-SIGN is differentially expressed in several tumor types (Figure 1A). Notably, DC-SIGN expression was significantly reduced in colorectal adenocarcinoma (COAD) tissues relative to adjacent normal tissues. This reduction may be attributed to the high immune cell infiltration typically observed in normal colon tissue.[26,27] Nevertheless, DC-SIGN expression levels in TCGA COAD remained comparable to those observed in other tumor types. Furthermore, using the ESTIMATE algorithm, we found a significant positive correlation between DC-SIGN expression and immune cell infiltration (Figure 1B).[28] Similarly, DC-SIGN expression was positively associated with stromal infiltration and overall ESTIMATE scores (Figures 1C and D), suggesting its relevance to the immune and stromal composition of the TME.

We further assessed the association between DC-SIGN expression and immune cell infiltration using the CIBERSORT algorithm.[29] Linear regression analysis revealed that DC-SIGN expression was positively correlated with M2-like macrophage infiltration but negatively correlated with M0 macrophages, consistent with its role as a recognized M2 macrophage marker (Figure 1D). In addition, DC-SIGN expression was inversely associated with the infiltration of activated mast cells and activated $CD4^+$ memory T cells (Figure 1E). Notably, no significant correlation was observed between DC-SIGN expression and $CD8^+$ T cell infiltration, suggesting that DC-SIGN may not directly modulate $CD8^+$ T cell responses in CRC tissues (Figure 1E). Moreover, DC-SIGN expression was not associated with clinical TNM stage (Figure 1F). Given its classification as an M2 macrophage marker, we compared the expression profile of DC-SIGN with that of another M2 marker, CD206, in CRC tissues. While CD206 similarly correlated with M2 macrophage infiltration, its association with M0 macrophages and mast cells differed from that of DC-SIGN (Supplementary Figure 1A). Furthermore, single-cell RNA-seq data from CRC samples demonstrated that DC-SIGN and CD206 are expressed in distinct macrophage subsets, with 33.26% (GSE132257) or 30.65% (GSE144735) of $CD206^+$ cells co-expressing DC-SIGN (Supplementary Figure 1B and C).

Upregulated DC-SIGN Expression is Associated with Unfavorable Prognosis in $CD8^{high}$ CRC Tumors

Next, we investigated the association between DC-SIGN expression and CRC prognosis. Patients with high versus low DC-SIGN-expressing CRC did not display a prognostic merit in the total TCGA COAD patients (Figures 2A and B). We reasoned that because DC-SIGN is mainly involved in tumor immune regulation, it may only elicit a role in tumor progression under proper immune microenvironment. As such, the COAD patients in the TCGA cohort were

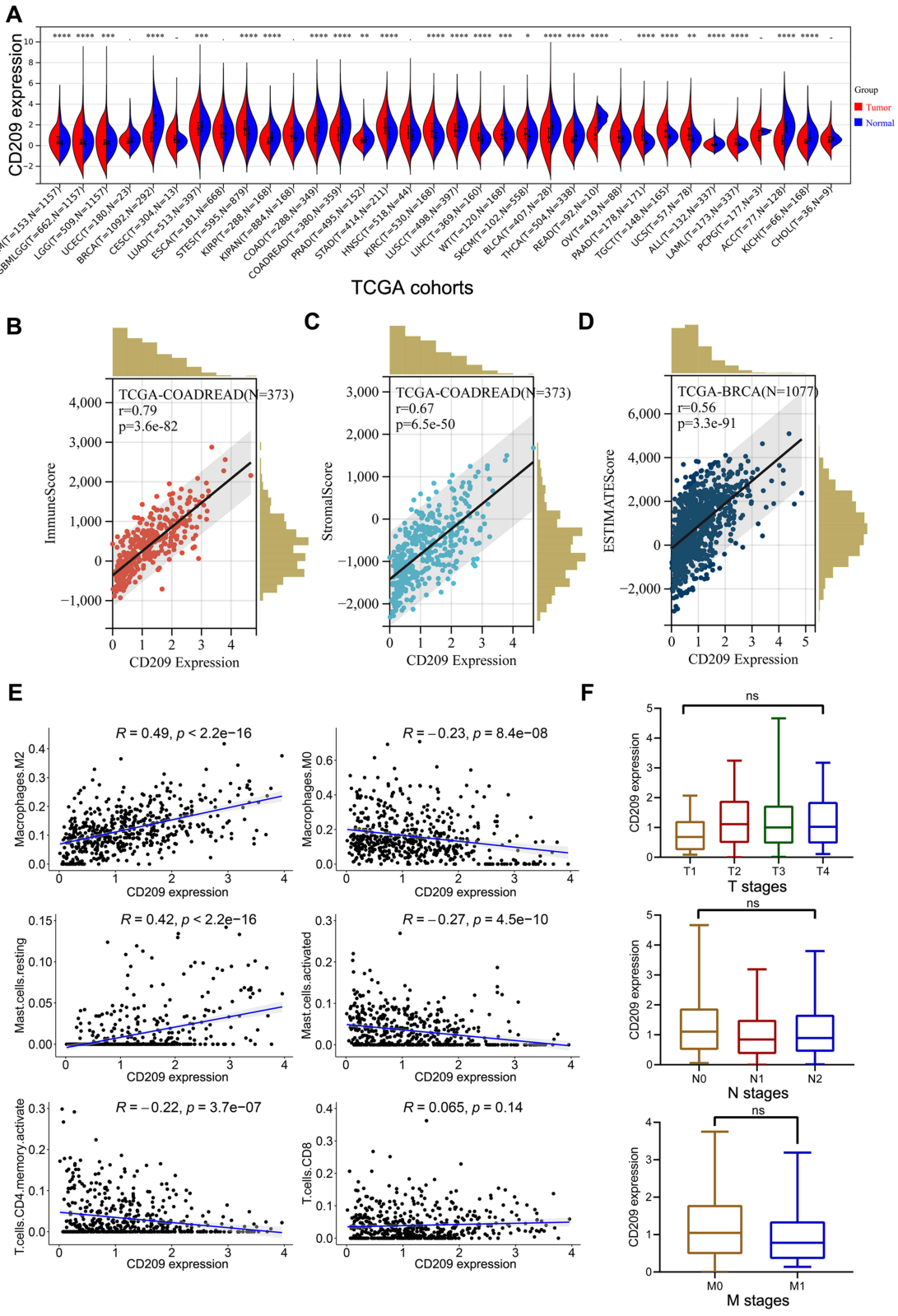

Figure 1 The association of DC-SIGN expression and CRC immune microenvironment. (**A**) Pan-cancer analysis of the differential expression of DC-SIGN between tumor and non-tumor tissues in TCGA database. (**B**) Pearson correlation between DC-SIGN expression and Immune Score in TCGA COADREAD dataset. (**C**) Pearson correlation between DC-SIGN expression and Stromalscore using the ESTIMATE algorithm. (**D**) Pearson correlation between DC-SIGN expression and ESTIMATE score. (**E**) Correlation of DC-SIGN expression and immune cell profiles. Immune cell profiles were estimated using the CIBERSORT algorithm. (**F**) DC-SIGN expression profiles across Tumor (T1-T4), Nodes (N0-N2) and Metastasis (M0-M1) stages in TCGA COADREAD samples. Statistical analyses were performed using Student's t-test (two groups) or one-way ANOVA (multiple groups). Significance is indicated as: ns (not significant), *P < 0.05, **P < 0.01, ***P < 0.001, ****P < 0.0001.

 https://doi.org/10.2147/ITT.S562182

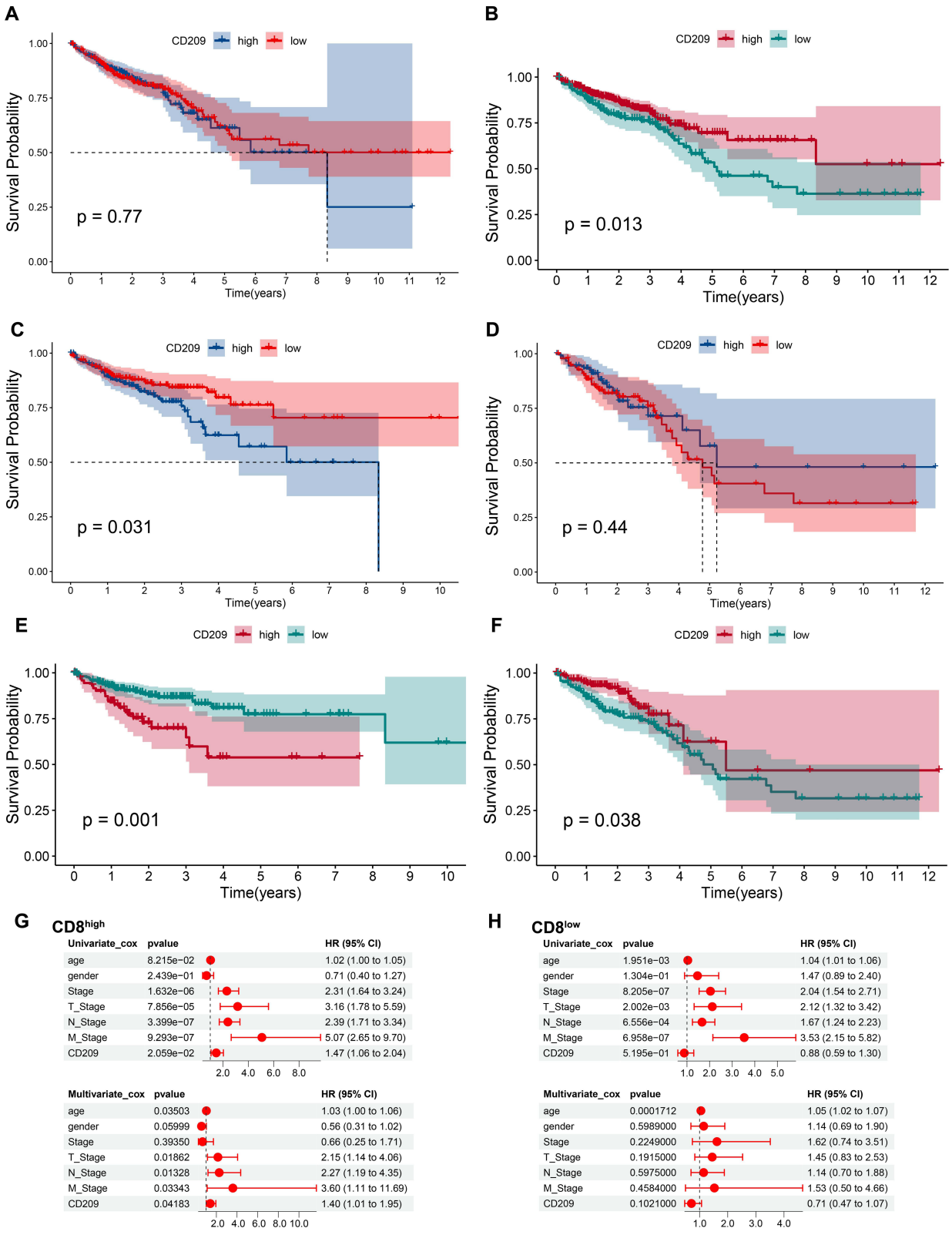

Figure 2 DC-SIGN expression is associated with unfavorable prognosis in immune-competent CRC tumors. (**A**–**F**) Kaplan-Meier curves of TCGA COADREAD dataset using median CD209 expression (**A, C** and **D**) or optimal CD209 expression (**B, E** and **F**). Patients were stratified into $CD8^{high}$ (**C** and **E**) or $CD8^{low}$ (**D** and **F**) using median CD8 expression as cut-off. (**G** and **H**) Univariable and multivariable Cox proportional hazards regression analyses of clinical parameters and DC-SIGN expression in $CD8^{high}$ (**G**) and $CD8^{low}$ (**H**) TCGA COADREAD group.

https://doi.org/10.2147/ITT.S562182

stratified into $CD8^{high}$ and $CD8^{low}$ groups, due to the fact that $CD8^+$ T cells play a determinant role in tumor immune elimination. When patients were stratified by median DC-SIGN expression, high DC-SIGN expression was associated with significantly worsened survival in the $CD8^{high}$ group. In contrast, no such association was observed in the $CD8^{low}$ (immune-depleted) group (Figures 2C and D). When the TCGA patient cohort was stratified by an optimal cut-off for DC-SIGN expression, the association with poor survival was more pronounced in immune-competent tumors (Figures 2E and F). When using univariate and multivariate Cox regression analysis, in the $CD8^{high}$ group, DC-SIGN expression served as an independent prognostic factor for evaluating the survival of patients (Figure 2G), while DC-SIGN expression was not prognostic in the immune-depleted group (Figure 2H).

DC-SIGN Expression is Specifically Associated with Worsened Prognosis in $CD8^{high}$ Patients

To further investigate the cellular source and clinical significance of DC-SIGN in CRC, we tested the hypothesis that its expression is confined to TAMs. To this end, CRC tissues collected from clinical settings were analyzed using dual immunofluorescence staining for CD68 and DC-SIGN (Figure 3A). Quantitative analysis of the immunofluorescence images revealed a significantly higher proportion of TAMs expressing DC-SIGN compared to those lacking DC-SIGN expression (Figure 3B). To further characterize these TAMs, single-cell suspensions were prepared from fresh clinical tumor tissues, and flow cytometry confirmed the specific expression of DC-SIGN on TAMs. The results demonstrated a high abundance of CD209-expressing TAMs in fresh CRC tissues (Figures 3C and D). Additionally, immunohistochemical staining for CD8 and DC-SIGN was conducted on CRC microarrays of the Nantong cohort. DC-SIGN expression was observed to be upregulated in regions with CD8 infiltration (Figure 3E).

High DC-SIGN Protein Expression Correlates with Poor Prognosis in $CD8^{high}$ Patients of the Nantong Cohort

Because TCGA cohort can only assess the prognostic values of DC-SIGN at mRNA level, we analyzed the prognostic merit of DC-SIGN expression in Nantong cohort. Following immunohistochemical analysis of DC-SIGN and CD8 expression in these tumor specimens, survival curves were drawn using median DC-SIGN expression. Similarly, we did not observe a clear prognostic value of DC-SIGN expression in the total patients (Supplementary Figure 2A). However, after grouping the clinical cohort according to CD8 expression, high DC-SIGN expression indicated a worse prognosis in the $CD8^{high}$ patients of the Nantong CRC cohort, whereas DC-SIGN expression is not prognostic in $CD8^{low}$ patients (Supplementary Figure 2B and C). DC-SIGN can be an independent prognostic factor for evaluating the prognosis of colorectal cancer (Supplementary Figure 2D). These findings explicitly support a role of $DC\text{-}SIGN^{high}$ TAMs in the regulation of CRC immunosuppressive environment and disease progression.

$DC\text{-}SIGN^{high}$ TAMs Display Unique Immune Pathway Profiles and Tumor Immune Checkpoint Expression

To investigate the gene expression profiles in groups with high and low DC-SIGN expression, we employed bioinformatics tools to analyze differential expression in the TCGA COADREAD cohort, identifying 1052 differentially expressed genes. These genes were subsequently subjected to GO and KEGG enrichment analyses to explore the biological processes and pathways associated with DC-SIGN.

As an antigen-presenting receptor, DC-SIGN is undeniably involved in regulating leukocyte and immune cell functions. Its molecular function is closely associated with antigen recognition and signal transduction receptor activity (Figure 4A). In KEGG enrichment analysis, we concentrated on tumor immunity-related pathways, including FcγR-mediated phagocytosis, PD-L1 expression and the PD-1 checkpoint pathway, NF-κB signaling, JAK-STAT signaling, IL-17 signaling, the C-type lectin receptor signaling pathway, Toll-like receptor signaling, and Th1/Th2 cell differentiation (Figure 4B). Additionally, we performed Gene Set Enrichment Analysis (GSEA) on these differentially expressed genes, revealing their primary roles in immune interactions between immune and non-immune cells, as well as in the adaptive immune system (Figure 4C). Differential gene expression was visualized using a heatmap (Figure 4D).

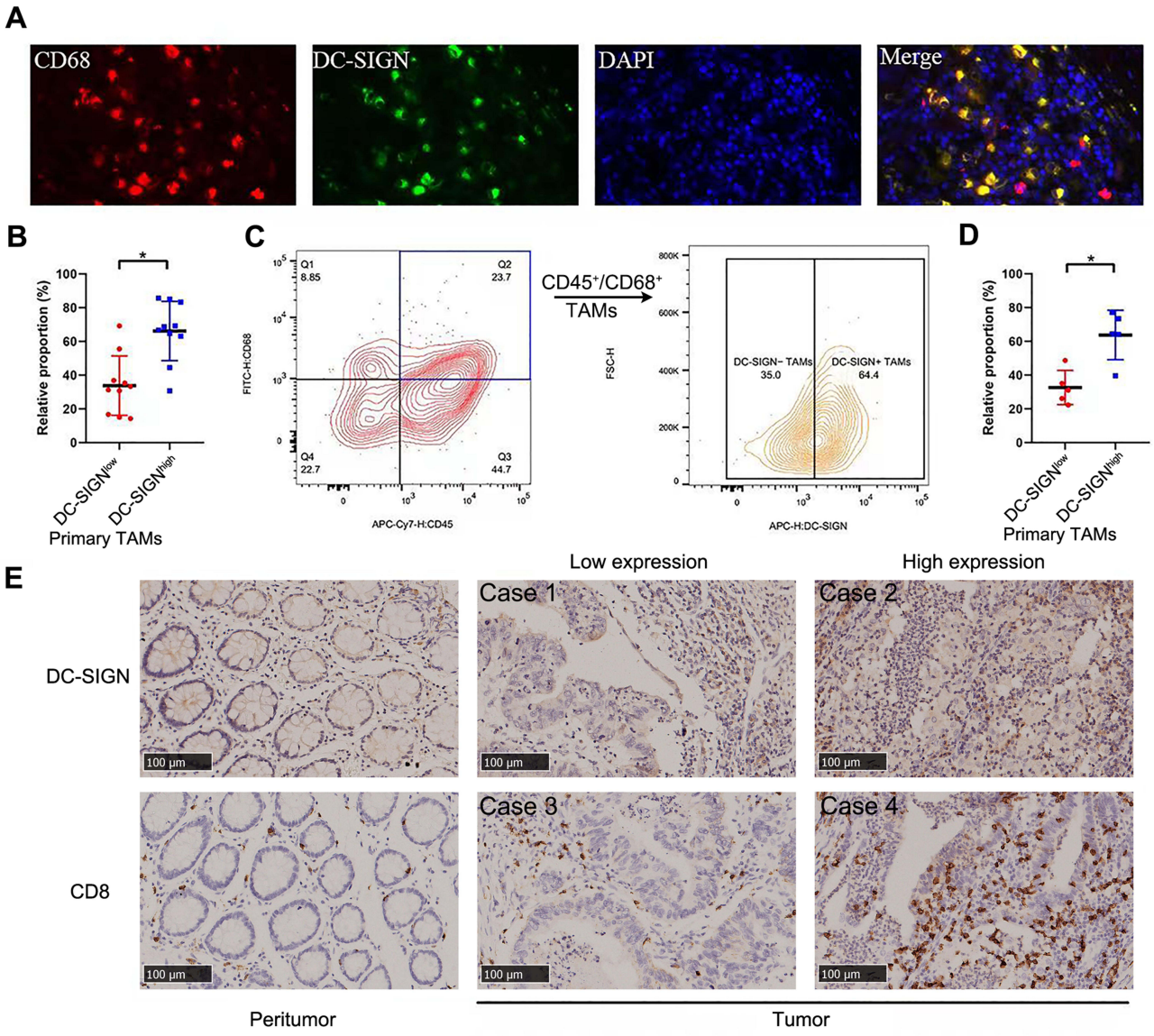

Figure 3 Characterization of DC-SIGN Expression in Tumor-Associated Macrophages in Colorectal Cancer. (**A**) Dual immunofluorescence staining showing the co-localization between DC-SIGN and CD68 in CRC tissues. (**B**) Differential distribution of DC-SIGN^{high} and DC-SIGN^{low} TAMs. (**C**) Flow cytometric analysis of DC-SIGN^{high} TAMs. CD45^{+}CD68^{+} TAMs were FACS-sorted from human colorectal cancer tissues. The resulting population was characterized for DC-SIGN expression. (**D**) Statistical analysis of DC-SIGN^{high} and DC-SIGN^{low} TAMs in flow cytometric analysis. (**E**) Representative immunohistochemical staining of DC-SIGN and CD8 expression in peritumor and CRC tissues. Statistical analyses were performed using Student's *t*-test. * $P < 0.05$.

DC-SIGN^{high} TAMs are Enriched with Tumor Immune Checkpoint PD-L1

To explore the gene expression differences between DC-SIGN^{+} and DC-SIGN^{-} TAMs, we performed RNA-seq on DC-SIGN^{high} and DC-SIGN^{low} TAMs sorted from single-cell suspensions of CRC tissues. TAMs from 4 fresh CRC tissues were collected for transcriptome analysis. A volcano plot of differential gene expression identified 52 significantly upregulated genes, including *DC-SIGN* and *CD274* (encoding PD-L1), as well as 690 significantly downregulated genes (Figure 5A).

Subsequent GO and KEGG enrichment analyses were performed to elucidate the functions of these differentially expressed genes and their associated pathways. GO analysis without stratification (Figure 5B) revealed that the upregulated genes were enriched in molecular functions related to scavenger receptors and toll-like receptors, likely reflecting responses to damage-associated molecular patterns (DAMPs) from cancer cells (Figure 5C). In contrast, the downregulated genes were enriched in cadherin binding, RAGE receptor binding, and ubiquitin-like protein binding. The

https://doi.org/10.2147/ITT.S562182

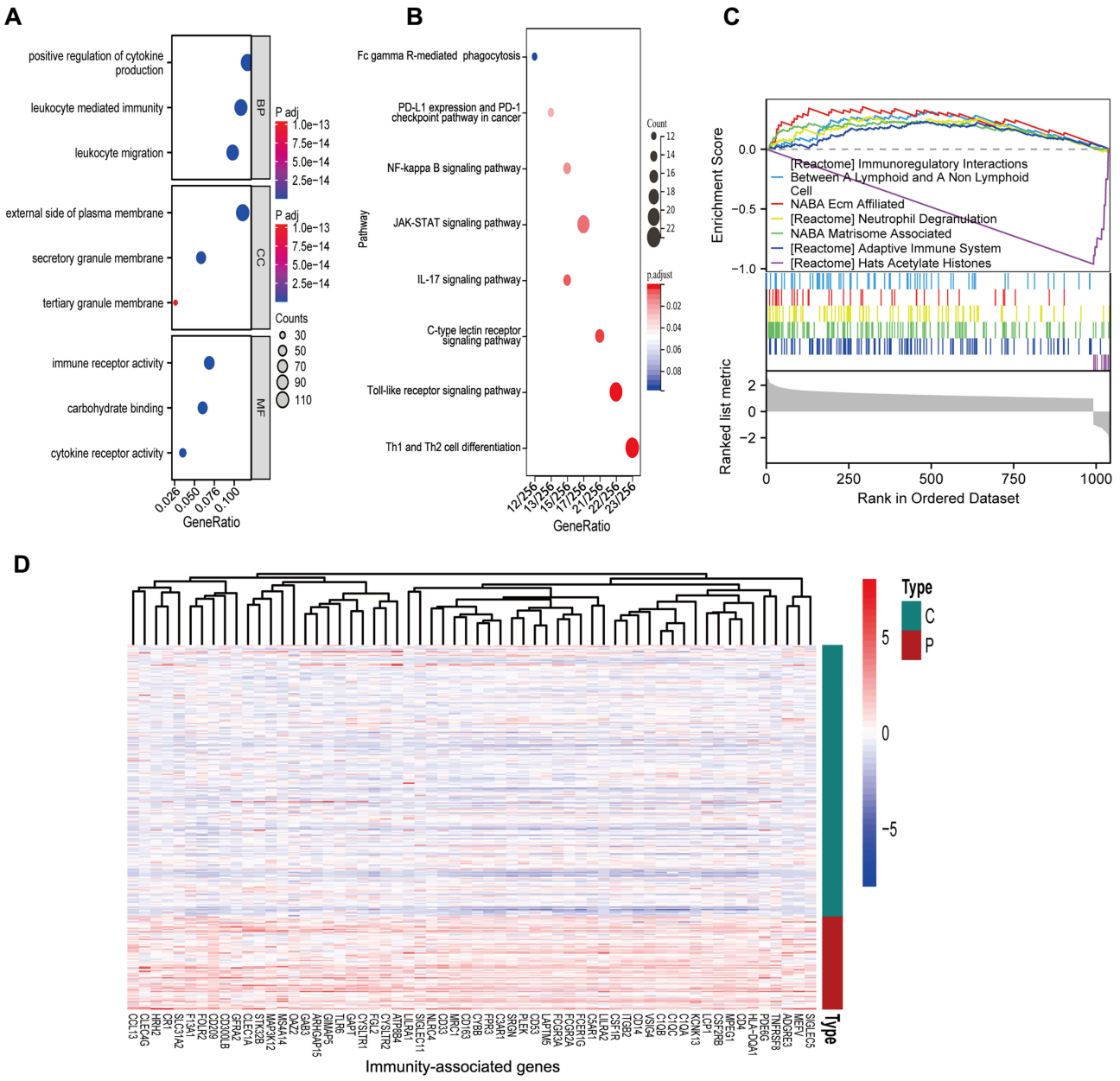

Figure 4 Differential Gene Expression and Bioinformatics Enrichment Analysis in DC-SIGN^{high} and DC-SIGN^{low} CRC groups. (**A**) GO enrichment analysis of differentially expressed genes in the TCGA COADREAD cohort. (**B**) KEGG enrichment analysis of differentially expressed genes in the TCGA COADREAD cohort. (**C**) GSEA results showing immune-related functions of differentially expressed genes. (**D**) Heatmap analysis of differentially expressed genes between DC-SIGN^{high} and DC-SIGN^{low} CRC samples.

associated biological processes included leukocyte aggregation, regulation of apoptosis signaling, granulocyte chemotaxis, neutrophil chemotaxis, and granulocyte migration, suggesting their involvement in tumor immune evasion (Figure 5D).

To identify genes potentially involved in the poor prognosis associated with DC-SIGN, we intersected differentially expressed genes from TCGA COADREAD with those obtained from our sequencing analysis, yielding 50 overlapping candidates. Among the upregulated genes, CD274 emerged as a prominent candidate (Figure 5E). In the TCGA cohort, DC-SIGN expression showed a strong positive correlation with CD274 mRNA levels (R = 0.6; Figure 5F). Consistently, single-cell RNA-seq data revealed significantly higher CD274 expression in DC-SIGN–positive (CD209_pos) TAMs compared to DC-SIGN–negative (CD209_neg) counterparts (Figure 5G). These findings suggest that DC-SIGN may

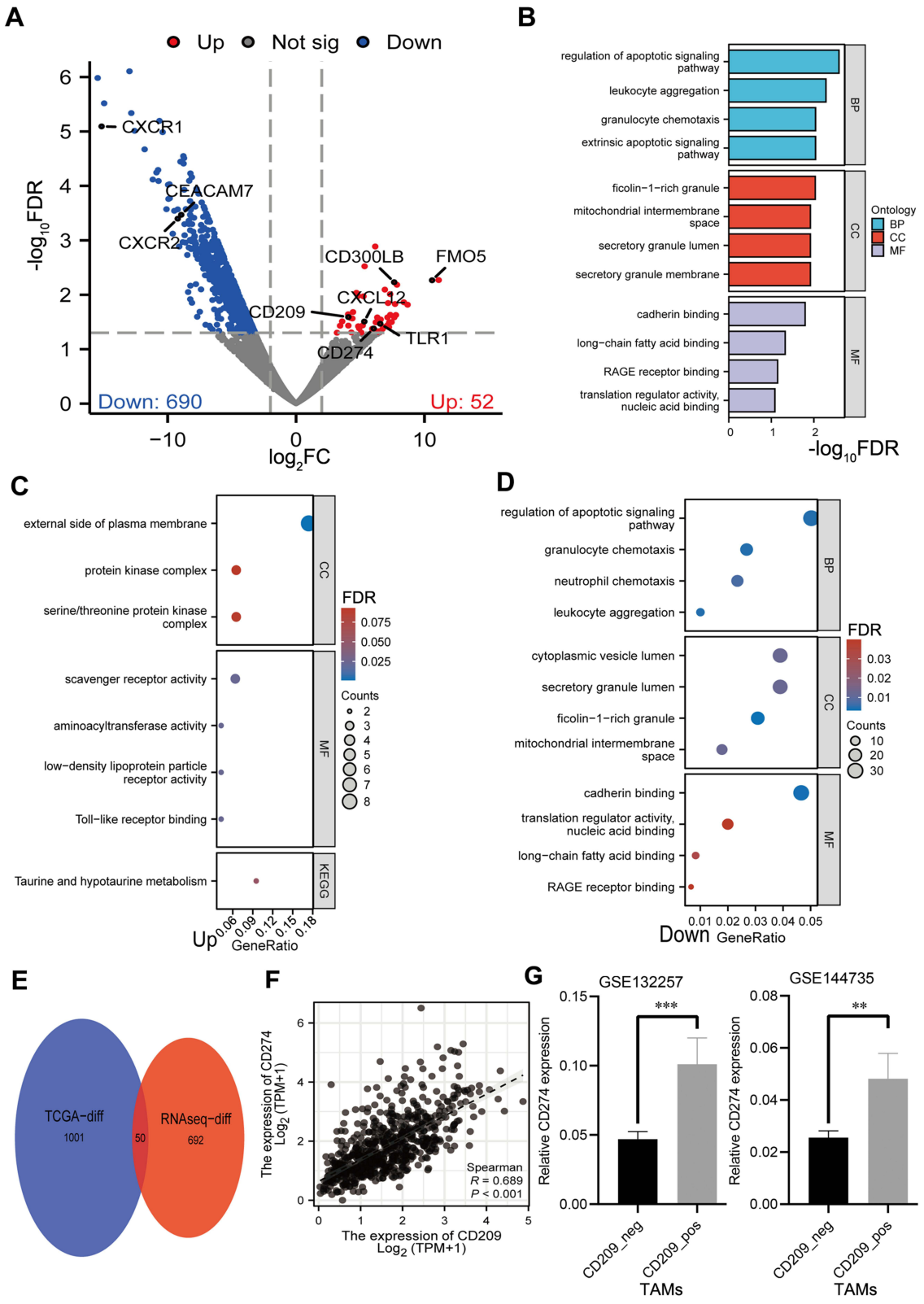

Figure 5 TAM-expressing DC-SIGN contributes to CD274/PD-L1 expression. (**A**) Volcano plot of differentially expressed genes in DC-SIGN^{high} vs DC-SIGN^{low} TAMs. (**B**) GO enrichment analysis of differentially expressed genes without stratification. (**C**) Enrichment analysis of upregulated genes. (**D**) Enrichment analysis of downregulated genes. (**E**) Venn diagram showing overlapping genes between TCGA COADREAD and sequencing results. (**F**) Correlation analysis between CD274 and DC-SIGN mRNA expression. (**G**) Comparison of CD274 mRNA expression between DC-SIGN–positive (CD209_pos) and DC-SIGN–negative (CD209_neg) TAMs in public single-cell RNA-seq data. Statistical analyses were performed using Student's *t*-test. ** $P < 0.01$, *** $P < 0.001$.

https://doi.org/10.2147/ITT.S562182

indirectly modulate tumor immunity by upregulating CD274, thereby promoting tumor progression and contributing to poor clinical outcomes.

DC-SIGN/BCL-3 Signaling Axis Directly Drives PD-L1 Expression in Macrophages

Our findings suggest a close correlation between DC-SIGN and PD-L1 expression in TAMs. To clarify the role of DC-SIGN signaling in regulating PD-L1 expression in macrophages, we employed THP-1-differentitated macrophages as cell model. Because IL-4 and IL-13 have been documented to drive the expression of DC-SIGN in human macrophages, we employed these cytokines to induce macrophage alternative polarization.[30] Following IL-4/13 treatment, macrophages exhibited significantly upregulated expression of DC-SIGN, as revealed by RT-qPCR assay (Figure 6A). Notably, we revealed that CD274 mRNA also showed considerable upregulation. This upregulation is validated by flow cytometry analysis showing over 2-fold increase in PD-L1 expression in IL-4/13-exposed macrophages (Figures 6B and C).

DC-SIGN has been shown to drive the activation of multiple NF-κB family transcription factors, particularly the non-canonical member BCL-3, by triggering the LSP1-IKKε-CYLD signaling cascade.[31] To investigate the involvement of BCL-3 in PD-L1 expression downstream of DC-SIGN, we examined whether BCL-3 has direct binding to the promoter of PD-L1 using ChIP-qPCR assay. We confirmed that BCL-3 directly binds to CD274 promoter and this binding was increased following Lewis^X (Le^X) stimulation (Figure 6D). Moreover, Le^X exposure caused significant upregulation of PD-L1 mRNA, whereas this upregulation can be abolished by BCL-3 interference (Figure 6E and Supplementary Figure 3). Moreover, flow cytometry analysis also demonstrated that Le^X facilitates PD-L1 expression via a BCL-3-dependent manner in macrophages (Figures 6F and G). When primary TAMs were stimulated with Le^X, the mRNA expression of PD-L1 was significantly upregulated (Figure 6H). These data suggest a causal role of DC-SIGN activation in PD-L1 expression in TAMs. Taken together, these findings indicate that DC-SIGN/BCL-3 signaling axis may directly activate PD-L1 expression in macrophages, highlighting this signaling pathway as a novel modulator of tumor immune checkpoint and immune evasion.

Discussion

Mounting evidence underscores the functional plasticity of TAMs, which can exhibit both pro-inflammatory and immunoregulatory properties within the TME.[32] This plasticity supports the concept that TAMs are highly heterogeneous and may be subclassified based on specific immune receptor expression. In this study, we demonstrated that TAMs classified by DC-SIGN expression exhibit distinct characteristics and prognostic significance. DC-SIGN^{high} TAMs uniquely influence the survival of patients with CD8^{high} CRC, indicating their role in regulating T-cell immunity in CRC. Additionally, TAMs sorting and RNA-seq analysis confirmed that DC-SIGN^{high} TAMs express high levels of genes involved in tumor immunity, particularly *CD274/PD-L1*. These findings strongly suggest that DC-SIGN^{high} TAMs play a critical role in immune regulation in CRC, underscoring their potential as a therapeutic target in CRC immunotherapy.[33]

TAMs are a major cellular constituent of the TIME, notable for their considerable morphological and functional diversity.[34,35] They play a pivotal role in fostering an immunosuppressive TIME that drives tumor immune evasion and resistance to immunotherapy, primarily through immune checkpoint pathways such as PD-L1/PD-1 and B7-CD28/CTLA-4.[36] Although the M1/M2-like categorization is frequently employed, this binary framework fails to capture the full heterogeneity of TAMs.[14] For instance, while M2-like TAMs are recognized as a major source of PD-L1 in tumor tissues, canonical M2 markers such as CD163 and CD206 have not been shown to directly regulate PD-L1.[37] Instead, PD-L1 expression is primarily driven by pro-inflammatory signals such as the JAK/STAT and NF-κB pathways.[38] Our work has defined DC-SIGN$^+$ TAMs as a distinct subpopulation and revealed their significant enrichment for PD-L1. Mechanistically, we found that the Le^X/DC-SIGN axis drives PD-L1 expression via an atypical NF-kB member BCL-3, highlighting the importance of this non-canonical regulatory axis in mediating CRC immune evasion.

In CRC, resistance to ICIs is closely linked to dynamic shifts in TAM phenotypes, positioning TAM reprogramming as a promising strategy to restore ICI sensitivity.[39] This concept is supported by the observed synergy and enhanced efficacy of combining colony-stimulating factor 1 receptor (CSF-1R) targeting with PD-1/PD-L1 blockade.[40,41] However, a systematic understanding of TAM plasticity in CRC remains limited, impeding the development of novel agents to overcome ICI resistance. Our findings establish a DC-SIGN-based TAM classification as a robust prognostic biomarker

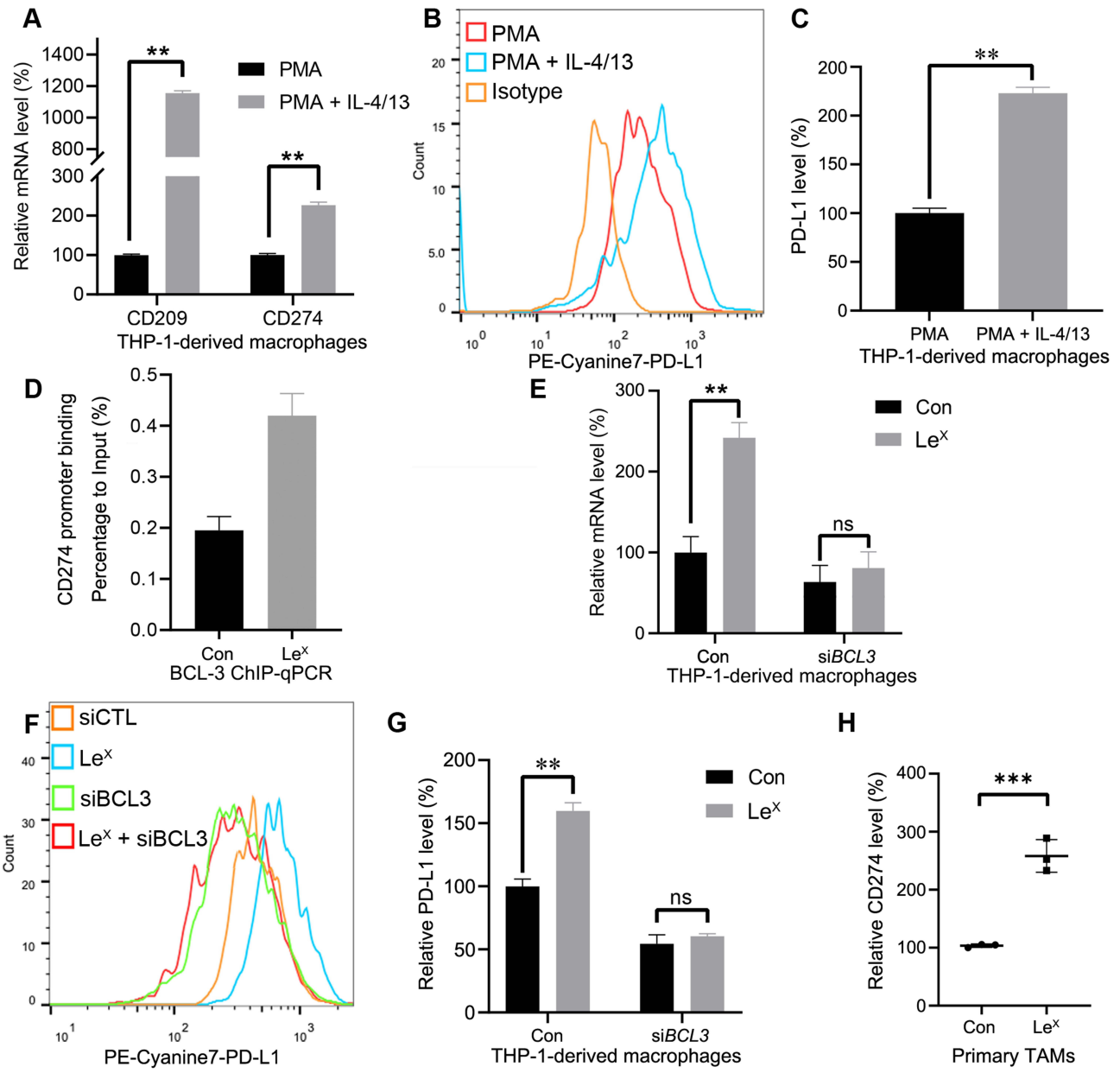

Figure 6 DC-SIGN/BCL-3 signaling axis directly drives PD-L1 expression in macrophages. (**A**) mRNA levels of DC-SIGN and CD274 in THP-1-differentiated macrophages in the absence or presence of IL-4/13 treatment. (**B**) Flow cytometry analysis of PD-L1 expression in macrophages with or without IL-4/13 exposure. (**C**) Statistical analysis of median PD-L1 level in the indicated groups. (**D**) ChIP-qPCR analysis of BCL-3 binding to CD274 promoter in THP-1-differentiated macrophages stimulated with or without Le^X. (**E**) RT-qPCR analysis of CD274 mRNA level in THP-1-differentiated macrophages following BCL-3 interference and Le^X exposure. (**F**) Flow cytometry analysis of PD-L1 level in THP-1-differentiated macrophages in the indicated groups. (**G**) Statistical analysis of median PD-L1 expression in macrophages. (**H**) RT-qPCR analysis of PD-L1 mRNA expression in DC-SIGN-expressing TAMs following mock (Con) or $Lewis^x$ (Le^X) exposure for 24 h. Statistical analyses were conducted using Student's *t*-test or two-way ANOVA. $^{ns}P > 0.05$, $^{**}P < 0.01$, $^{***}P < 0.001$.

for $CD8^{high}$ CRC. Moreover, we mechanistically demonstrate that DC-SIGN directly drives PD-L1 expression in TAMs, nominating it as a promising therapeutic target for overcoming ICI resistance.

DC-SIGN is a C-type lectin receptor that specifically recognizes Lewis antigens and is critically implicated in immune evasion across viral infections and cancers.[42] Studies have shown that this receptor has the ability to bind to enriched Lewis antigens on carcinoembryonic antigen (CEA) within CRC tissues, which may suppress anti-tumor T cell responses.[15] Furthermore, glycoproteins carrying DC-SIGN-activating Lewis glycans, such as Mac-2-binding protein (Mac-2BP) and Mucin 1 (MUC1), are highly abundant in CRC tissues.[20,43] This abundance of ligands creates a persistent signal that fuels DC-SIGN activation, establishing a glycan-driven layer of immune suppression. While DC-SIGN is

https://doi.org/10.2147/ITT.S562182

reportedly expressed in DCs and macrophages, our data demonstrate its predominant expression on a specific subset of TAMs within CRC. We further identified a significant infiltration of these DC-SIGN^{high} TAMs in a large proportion of CRC specimens. Transcriptomic analysis linked this TAM subpopulation to significant enrichments in unique tumor-associated immune pathways, including the PD-L1 immune checkpoint pathway. These findings highlight DC-SIGN^{high} TAMs as a crucial immune cell population actively engaged in CRC tumor evasion.

Using integrative approaches, including flow cytometry, immunofluorescence, and RNA-seq, we identified DC-SIGN^{high} TAMs as a pivotal immune population in the TME of clinical CRC specimens. Notably, the abundance of DC-SIGN^{high} TAMs selectively correlates with poor prognosis specifically in patients with high levels of $CD8^+$ cytotoxic T lymphocytes (CTLs), a context typically associated with immunologically "hot" tumors and higher responsiveness to immunotherapy.[44,45] Mechanistically, we linked this association to PD-L1 expression in DC-SIGN^{high} TAMs. DC-SIGN activation by its natural ligand Le^X robustly enhances PD-L1 expression at both mRNA and protein levels in macrophages. Furthermore, we showed that DC-SIGN facilitates PD-L1 upregulation via BCL-3-mediated transcription. Importantly, our ChIP-qPCR and ChIP-seq data from the ENCODE project confirmed a direct binding of BCL-3 to CD274 promoter.[46] These results nominate the DC-SIGN/BCL-3 axis as a potential therapeutic target for cancer immunotherapy.

Previous studies have identified DC-SIGN and BCL-3 as promising therapeutic targets for cancer treatment. As an immune receptor on the cell membrane, DC-SIGN has been targeted by neutralizing antibodies, which have demonstrated potent efficacy in blocking its function and enhancing anti-tumor immunity.[23] The development of such antibodies, along with antibody-drug conjugates (ADCs), may open new avenues for novel tumor immunotherapy.[47] Meanwhile, BCL-3 has been shown to function both as a modulator of the TIME and as an oncogenic driver in CRC cells, where it promotes stemness, chemoresistance, and invasion.[48–50] Notably, the anti-inflammatory agent 5-aminosalicylic acid (5-ASA) can suppress BCL-3 expression in CRC cells.[51] Furthermore, the BCL-3–specific inhibitors JS6 and A27 disrupt the BCL-3–NF-κB1 interaction and demonstrate anti-tumor efficacy.[52,53] Although these findings are still preliminary, they highlight the translational potential of targeting BCL-3 to simultaneously inhibit CRC progression and synergize with immune checkpoint blockade.

In summary, our study establishes DC-SIGN^{high} TAMs as an independent prognostic factor in CRC and reveals their critical immunosuppressive role, which is mechanistically underpinned by BCL-3-driven PD-L1 upregulation. These findings provide a mechanistic foundation for targeting the DC-SIGN/BCL-3/PD-L1 axis, presenting a promising strategic avenue for advancing anti-TAM immunotherapy in CRC treatment.

Data Sharing Statement

The datasets used and analyzed in this study are available from the corresponding author (Fei Qian) on reasonable request.

Ethics Approval and Informed Consent

The study was conducted in accordance with the Declaration of Helsinki, and approved by Ethics Committee of Affiliated Hospital of Nantong University (Ethics number 2020-K091-01). Formal written consent forms were received from all patients enrolled in this study.

Funding

This work was supported by grants from the National Natural Science Foundation of China (82273206), Jiangsu Provincial Research Hospital (YJXYY202204-2-YSC18, YJXYY202204-2-YSB24), Nantong Science and Technology Project (MS2024041).

Disclosure

Jianfeng Zhang and Yifan Zhao contributed equally to this work and share first authorship. The authors have no conflicts of interest to declare.

References

1. Han B, Zheng R, Zeng H, et al. Cancer incidence and mortality in China, 2022. *J Natl Cancer Cent*. 2024;4(1):47–53. doi:10.1016/j.jncc.2024.01.006
2. Wang Y, Zhang Z, Sun W, et al. Ferroptosis in colorectal cancer: potential mechanisms and effective therapeutic targets. *Biomed Pharmacother*. 2022;153:113524. doi:10.1016/j.biopha.2022.113524
3. Siegel RL, Miller KD, Wagle NS, et al. Cancer statistics, 2023. *CA Cancer J Clin*. 2023;73(1):17–48. doi:10.3322/caac.21763
4. Argilés G, Tabernero J, Labianca R, et al. Localised colon cancer: ESMO clinical practice guidelines for diagnosis, treatment and follow-up. *Ann Oncol*. 2020;31(10):1291–1305. doi:10.1016/j.annonc.2020.06.022
5. Zhu C, Han G, Wu B. Cost-effectiveness analysis of pembrolizumab versus chemotherapy as first-line treatment for mismatch-repair-deficient (dMMR) or microsatellite-instability-high (MSI-H) advanced or metastatic colorectal cancer from the perspective of the Chinese health-care system. *BMC Health Serv Res*. 2023;23(1):1083. doi:10.1186/s12913-023-10037-1
6. Chen D, Wang H. The clinical and immune features of CD14 in colorectal cancer identified via large-scale analysis. *Int Immunopharmacol*. 2020;88:106966. doi:10.1016/j.intimp.2020.106966
7. Haslam A, Prasad V. Estimation of the percentage of US patients with cancer who are eligible for and respond to checkpoint inhibitor immunotherapy drugs. *JAMA Network Open*. 2019;2(5):e192535. doi:10.1001/jamanetworkopen.2019.2535
8. Zhang L, Maalouf A, Makri SC, et al. Multidimensional immunotyping of human NF1-associated peripheral nerve sheath tumors uncovers tumor-associated macrophages as key drivers of immune evasion in the tumor microenvironment. *Clin Cancer Res*. 2024;30(23):5459–5472. doi:10.1158/1078-0432.CCR-24-1454
9. Yu Y, Liu M, Wang Z, et al. Identification of oxidative stress signatures of lung adenocarcinoma and prediction of patient prognosis or treatment response with single-cell RNA sequencing and bulk RNA sequencing data. *Int Immunopharmacol*. 2024;137:112495. doi:10.1016/j.intimp.2024.112495
10. Kumari N, Choi SH. Tumor-associated macrophages in cancer: recent advancements in cancer nanoimmunotherapies. *J Exp Clin Cancer Res*. 2022;41(1):68. doi:10.1186/s13046-022-02272-x
11. Yin Y, Yao S, Hu Y, et al. The immune-microenvironment confers chemoresistance of colorectal cancer through macrophage-derived IL6. *Clin Cancer Res*. 2017;23(23):7375–7387. doi:10.1158/1078-0432.CCR-17-1283
12. Gordon SR, Maute RL, Dulken BW, et al. PD-1 expression by tumour-associated macrophages inhibits phagocytosis and tumour immunity. *Nature*. 2017;545(7655):495–499. doi:10.1038/nature22396
13. Yin Y, Liu B, Cao Y, et al. Colorectal cancer-derived small extracellular vesicles promote tumor immune evasion by upregulating PD-L1 expression in tumor-associated macrophages. *Adv Sci*. 2022;9(9):2102620. doi:10.1002/advs.202102620
14. Nasir I, McGuinness C, Poh AR, et al. Tumor macrophage functional heterogeneity can inform the development of novel cancer therapies. *Trends Immunol*. 2023;44(12):971–985. doi:10.1016/j.it.2023.10.007
15. van Gisbergen KP, Aarnoudse CA, Meijer GA, et al. Dendritic cells recognize tumor-specific glycosylation of carcinoembryonic antigen on colorectal cancer cells through dendritic cell-specific intercellular adhesion molecule-3-grabbing nonintegrin. *Cancer Res*. 2005;65(13):5935–5944. doi:10.1158/0008-5472.CAN-04-4140
16. Zhou T, Chen Y, Hao L, et al. DC-SIGN and immunoregulation. *Cell Mol Immunol*. 2006;3(4):279–283.
17. Liu X, Cao Y, Li R, et al. Poor clinical outcomes of intratumoral dendritic cell-specific intercellular adhesion molecule 3-grabbing non-integrin-positive macrophages associated with immune evasion in gastric cancer. *Eur J Cancer*. 2020;128:27–37. doi:10.1016/j.ejca.2020.01.002
18. Yan X, Li W, Pan L, et al. Lewis lung cancer cells promote SIGNR1(CD209b)-mediated macrophages polarization induced by IL-4 to facilitate immune evasion. *J Cell Biochem*. 2016;117(5):1158–1166. doi:10.1002/jcb.25399
19. Merlotti A, Malizia AL, Michea P, et al. Aberrant fucosylation enables breast cancer clusterin to interact with dendritic cell-specific ICAM-grabbing non-integrin (DC-SIGN). *Oncoimmunology*. 2019;8(9):e1629257. doi:10.1080/2162402X.2019.1629257
20. Nonaka M, Ma BY, Imaeda H, et al. Dendritic cell-specific intercellular adhesion molecule 3-grabbing non-integrin (DC-SIGN) recognizes a novel ligand, Mac-2-binding protein, characteristically expressed on human colorectal carcinomas. *J Biol Chem*. 2011;286(25):22403–22413. doi:10.1074/jbc.M110.215301
21. Nonaka M, Ma BY, Murai R, et al. Glycosylation-dependent interactions of C-type lectin DC-SIGN with colorectal tumor-associated Lewis glycans impair the function and differentiation of monocyte-derived dendritic cells. *J Immunol*. 2008;180(5):3347–3356. doi:10.4049/jimmunol.180.5.3347
22. Melero I, Gabari I, Corbí AL, et al. An anti-ICAM-2 (CD102) monoclonal antibody induces immune-mediated regressions of transplanted ICAM-2-negative colon carcinomas. *Cancer Res*. 2002;62(11):3167–3174.
23. Hu B, Wang Z, Zeng H, et al. Blockade of DC-SIGN(+) tumor-associated macrophages reactivates antitumor immunity and improves immunotherapy in muscle-invasive bladder cancer. *Cancer Res*. 2020;80(8):1707–1719. doi:10.1158/0008-5472.CAN-19-2254
24. Wang X, Zhang J, Hu B, et al. High expression of CSF-1R predicts poor prognosis and CSF-1R(high) tumor-associated macrophages inhibit anti-tumor immunity in colon adenocarcinoma. *Front Oncol*. 2022;12:850767. doi:10.3389/fonc.2022.850767
25. Newman AM, Liu CL, Green MR, et al. Robust enumeration of cell subsets from tissue expression profiles. *Nat Methods*. 2015;12(5):453–457. doi:10.1038/nmeth.3337
26. Parikh K, Antanaviciute A, Fawkner-Corbett D, et al. Colonic epithelial cell diversity in health and inflammatory bowel disease. *Nature*. 2019;567(7746):49–55. doi:10.1038/s41586-019-0992-y
27. Peterson LW, Artis D. Intestinal epithelial cells: regulators of barrier function and immune homeostasis. *Nat Rev Immunol*. 2014;14(3):141–153. doi:10.1038/nri3608
28. Yoshihara K, Shahmoradgoli M, Martínez E, et al. Inferring tumour purity and stromal and immune cell admixture from expression data. *Nat Commun*. 2013;4(1):2612. doi:10.1038/ncomms3612
29. Chen B, Khodadoust MS, Liu CL, Newman AM, Alizadeh AA. Profiling tumor infiltrating immune cells with CIBERSORT. *Methods Mol Biol*. 2018;1711:243–259.
30. Rogers KJ, Brunton B, Mallinger L, et al. IL-4/IL-13 polarization of macrophages enhances Ebola virus glycoprotein-dependent infection. *PLoS Negl Trop Dis*. 2019;13(12):e0007819. doi:10.1371/journal.pntd.0007819

31. Gringhuis SI, Kaptein TM, Wevers BA, et al. Fucose-specific DC-SIGN signalling directs T helper cell type-2 responses via IKKε- and CYLD-dependent Bcl3 activation. *Nat Commun*. 2014;5(1):3898. doi:10.1038/ncomms4898
32. Murray PJ, Allen J, Biswas S, et al. Macrophage activation and polarization: nomenclature and experimental guidelines. *Immunity*. 2014;41(1):14–20. doi:10.1016/j.immuni.2014.06.008
33. Bouma RG, Nijen Twilhaar MK, Brink HJ, et al. Nanobody-liposomes as novel cancer vaccine platform to efficiently stimulate T cell immunity. *Int J Pharm*. 2024;660:124254. doi:10.1016/j.ijpharm.2024.124254
34. Zhao Y, Ni Q, Zhang W, et al. Progress in reeducating tumor-associated macrophages in tumor microenvironment. *Discov Oncol*. 2024;15(1):312. doi:10.1007/s12672-024-01186-8
35. Dong Q, Zhang S, Zhang H, et al. MARCO is a potential prognostic and immunotherapy biomarker. *Int Immunopharmacol*. 2023;116:109783. doi:10.1016/j.intimp.2023.109783
36. Yu Y, Liang Y, Xie F, et al. Tumor-associated macrophage enhances PD-L1-mediated immune escape of bladder cancer through PKM2 dimer-STAT3 complex nuclear translocation. *Cancer Lett*. 2024;593:216964. doi:10.1016/j.canlet.2024.216964
37. Boutilier AJ, Elsawa SF. Macrophage Polarization States in the Tumor Microenvironment. *Int J Mol Sci*. 2021;22(13):6995. doi:10.3390/ijms22136995
38. Kumar S, Sharawat SK. Epigenetic regulators of programmed death-ligand 1 expression in human cancers. *Transl Res*. 2018;202:129–145. doi:10.1016/j.trsl.2018.05.011
39. Cheruku S, Rao V, Pandey R, et al. Tumor-associated macrophages employ immunoediting mechanisms in colorectal tumor progression: current research in Macrophage repolarization immunotherapy. *Int Immunopharmacol*. 2023;116:109569. doi:10.1016/j.intimp.2022.109569
40. Lv Q, Yang H, Wang D, et al. Discovery of a novel CSF-1R inhibitor with highly improved pharmacokinetic profiles and superior efficacy in colorectal cancer immunotherapy. *J Med Chem*. 2024;67(8):6854–6879. doi:10.1021/acs.jmedchem.4c00508
41. Shimizu D, Yuge R, Kitadai Y, et al. Pexidartinib and immune checkpoint inhibitors combine to activate tumor immunity in a murine colorectal cancer model by depleting M2 macrophages differentiated by cancer-associated fibroblasts. *Int J Mol Sci*. 2024;25(13):7001. doi:10.3390/ijms25137001
42. Kremsreiter SM, Kroell A-SH, Weinberger K, et al. Glycan-lectin interactions in cancer and viral infections and how to disrupt them. *Int J Mol Sci*. 2021;22(19):10577. doi:10.3390/ijms221910577
43. Saeland E, Belo AI, Mongera S, et al. Differential glycosylation of MUC1 and CEACAM5 between normal mucosa and tumour tissue of colon cancer patients. *Int J Cancer*. 2012;131(1):117–128. doi:10.1002/ijc.26354
44. Appleton E, Hassan J, Chan Wah Hak C, et al. Kickstarting immunity in cold tumours: localised tumour therapy combinations with immune checkpoint blockade. *Front Immunol*. 2021;12:754436. doi:10.3389/fimmu.2021.754436
45. Wang Q, Qin Y, Li B. CD8(+) T cell exhaustion and cancer immunotherapy. *Cancer Lett*. 2023;559:216043. doi:10.1016/j.canlet.2022.216043
46. Consortium EP. An integrated encyclopedia of DNA elements in the human genome. *Nature*. 2012;489(7414):57–74.
47. Alonso MN, Gregorio JG, Davidson MG, et al. Depletion of inflammatory dendritic cells with anti-CD209 conjugated to saporin toxin. *Immunol Res*. 2014;58(2–3):374–377. doi:10.1007/s12026-014-8511-6
48. Legge DN, Shephard AP, Collard TJ, et al. BCL-3 promotes a cancer stem cell phenotype by enhancing β-catenin signalling in colorectal tumour cells. *Dis Model Mech*. 2019;12(3):dmm037697.
49. Parker C, Chambers AC, Flanagan DJ, et al. BCL-3 loss sensitises colorectal cancer cells to DNA damage by targeting homologous recombination". *DNA Repair*. 2022;115:103331. doi:10.1016/j.dnarep.2022.103331
50. Legge DN, Chambers AC, Parker CT, et al. The role of B-Cell Lymphoma-3 (BCL-3) in enabling the hallmarks of cancer: implications for the treatment of colorectal carcinogenesis. *Carcinogenesis*. 2020;41(3):249–256. doi:10.1093/carcin/bgaa003
51. Urban BC, Collard TJ, Eagle CJ, et al. BCL-3 expression promotes colorectal tumorigenesis through activation of AKT signalling. *Gut*. 2016;65(7):1151–1164. doi:10.1136/gutjnl-2014-308270
52. Soukupová J, Bordoni C, Turnham DJ, et al. The discovery of a novel antimetastatic Bcl3 inhibitor. *Mol Cancer Ther*. 2021;20(5):775–786. doi:10.1158/1535-7163.MCT-20-0283
53. Saamarthy K, Daams R, Sime W, et al. An optimised Bcl-3 inhibitor for melanoma treatment. *Br J Pharmacol*. 2025;182(11):2426–2446. doi:10.1111/bph.17467